Electron Emission from Mesonic Atoms*

G. T. CONDO,† R. D. HILL, AND A. D. MARTIN‡
Physics Department, University of Illinois, Urbana, Illinois
(Received 5 September 1963)

The yield and energy distribution of electrons emitted from absorptions of stopping K^- mesons in nuclear emulsions have been measured. In the electron energy range from 20–70 keV, the yield in the heavy elements Ag and Br has been analyzed to consist of 14% background electrons contributed by radioactivity, and 24% contributed by the radiationless Auger process in the K-mesonic atom. This Auger yield is considerably less than would be expected theoretically from existing conventional analyses of the K^--mesonic atom cascade in Ag and Br. A possible explanation of the discrepancy is given in terms of a description involving Stark mixing in highly excited mesonic states. This gives rise to nuclear capture from the f and d angular momentum substates of highly excited levels. The probable effect of such a capture mechanism on the rate of multinucleon captures in nuclei is briefly discussed. Further experimental results are given on electron emission from π-mesonic atoms, and other data on μ-mesonic and Σ-hyperonic atoms are also reviewed.

I. INTRODUCTION

WHEN negative heavy particles (such as μ^-, π^-, K^-, Σ^-) are arrested in matter, provided their lifetimes are sufficiently long, they quickly become captured by atoms of the material. An atom in which the meson has become locally captured is known by the generic title of a mesonic atom. Since the discovery of negative mesons nearly two decades ago, considerable interest has been attached to the properties of mesonic atoms. Only recently has the problem of capture and subsequent cascade of negative mesons bound to protons in liquid hydrogen been well understood.[1] It is the purpose of the present investigation to attempt a fuller description of the de-excitation of complex mesonic atoms. This de-excitation occurs by both radiative and nonradiative processes. The mesonic Auger process, whereby a meson de-excites by concurrent ejection from the mesonic atom of an atomic electron, is the dominant nonradiative process.

Experimental evidence on electron emission from mesonic atoms will be presented in the first part of the paper. The main body of the text will deal exclusively with K^- mesons captured in AgBr crystals of nuclear emulsion and the second part of the paper will deal with theoretical interpretations of the K^--mesonic atom cascades. In an Appendix, an experiment on π^--mesonic atoms is described and the current status of electron emission from μ^--mesonic and Σ^--hyperonic atoms is outlined. Although the main discussion is confined to K^--mesonic atoms, the general conclusions should be applicable, with appropriate modifications, to other types of mesonic atoms.

* The work of one of us (A.D.M.) was supported by the U. S. Office of Naval Research. For a part of the time, the work of the others (G.T.C. and R.D.H.) was supported by the Office of Naval Research, and since October 1962, was supported by the U. S. Atomic Energy Commission under Contract AT(11-1)-1195.

† Present address: Physics Department, University of Tennessee, Knoxville, Tennessee.

‡ Present address: National Institute for Research in Nuclear Science, Harwell, England.

[1] T. B. Day, G. A. Snow, and J. Sucher, Phys. Rev. Letters **3**, 61 (1959); M. Leon and H. A. Bethe, Phys. Rev. **127**, 636 (1962).

II. EXPERIMENTAL STUDY OF K^--MESONIC ATOMS

A sample of 2190 K^- stars located in electron sensitive G5 emulsion was chosen for a study of the mesonic Auger effect. The K^- stopping tracks were identified by ionization measurements. Each star was carefully examined for the presence of electrons of energies ≥ 20 keV emerging from the vertex of the star. (The minimum energy of 20 keV was chosen because Martin's[2] theoretical spectrum only extends down to this value and because such a relatively high energy value tends to minimize any contamination from incorrectly classified short nuclear recoils and blobs.) The range of a 20-keV electron in normal G5 emulsion is approximately 3 μ. Demer's[3] composite range-energy relation has been used throughout the present work.

The K^--capture events were separated into captures by the heavy atoms of the emulsion, Ag and Br, and by the light elements, C, N, O. In order to effect this separation, the method of short prongs was invoked; i.e., the emission of a short prong or recoil of range $2\,\mu \leq R \leq 46\,\mu$ was taken to imply that the capture occurred on a light nucleus. In the present experiments it was found that 63% of the K^- captures occurred in the heavy elements, Ag and Br.

Of the 1380 K^- captures in the heavy nuclei, it has been observed that there were 575 low-energy electrons (≥ 20 keV) emitted. This number of electrons does not distinguish between K^--capture events in which only one and more than one electron was emitted. In other words, if two electrons were emitted from a single star both were counted in the total. (This method of counting will be adopted throughout this work and when an Auger yield is expressed as a percentage, it is to be taken as the total number of electrons emitted divided by the total number of K-meson captures in the nuclei concerned.) For the light nuclei, there were only 35 electrons (≥ 20 keV) in 810 events. Thus, the frequency of low-energy electron emission for K^--mesonic atoms

[2] A. D. Martin, Nuovo Cimento **27**, 1359 (1963).

[3] P. Demers, *Ionographie, Les Emulsions Nucléaires: Principes et applications* (Les Presses Universitaires, Montreal, 1948), p. 250.

was found to be 0.42 for heavy nuclei and 0.04 for light nuclei. These results are compared with those obtained in other laboratories in Table I.[4–12]

From Table I, it is seen that, considering the different low-energy electron cutoffs employed, the results from many different workers are in reasonably good agreement. (The cutoff of 10 keV used by Csejthey-Barth and Sacton[5] probably accounts for the comparatively high value of 0.65 for their electron frequency from heavy nuclei. These authors separated electrons from blobs and their value is therefore not directly comparable with the value obtained by Eisenberg and Kessler.[7])

In Figs. 1 and 2 are presented the observed energy spectra of electrons emitted from K^- captures in. heavy nuclei. No measurements are given beyond 120 keV because errors are expected to be large. These arise because high-energy electron tracks become difficult to follow due to scattering and low ionization. The worst disturbance in the energy determination lies in the range straggling of the order of 25% for electron tracks.[9,13] This makes the delineation of the low-energy Auger electron spectrum in nuclear emulsion exceedingly difficult. Similar experimental spectra have been obtained by Chesick and Schneps,[4] by Condo,[14] and by Eisenberg and Kessler.[7]

Of special interest are the electron emission fre-

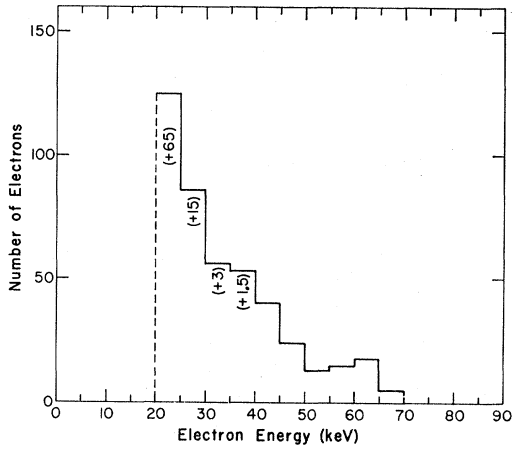

FIG. 1. Observed electron-energy spectrum (20–70 keV) for K^--mesonic atoms. An experimental cutoff was used below 20 keV. Numbers in parenthesis are to be added as corrections to the numbers already in the assigned energy bins; they represent losses attributable to the geometrical factor described in footnote (g) of Table I.

TABLE I. Summary of experimental observations on electron emission from K^- stars.

Investigators	Number of K^- events	Minimum energy (keV)	Fraction of captures on Ag and Br	Heavy nucleus electron emission frequency
Chesick and Schneps[a]	195	15	0.63[b]	0.63
Grote *et al.*[c]	1000	~13	0.75	0.33±0.03
Csejthey-Barth and Sacton[d]	1174	10	0.58	0.65±0.07
Eisenberg and Kessler[e]	278	15	0.57	~1.3[f]
Present work	2190	20	0.63	0.42 (0.48)[g]

[a] See Ref. 4.
[b] In order to obtain a value of the electron-emission frequency from the work of Chesick and Schneps (Ref. 4) we have assumed that the fraction of nuclear captures in Ag and Br is 0.63.
[c] See Ref. 5.
[d] See Ref. 6.
[e] See Ref. 7.
[f] Eisenberg and Kessler (Ref. 7) include all blobs as well as electrons in their electron frequency. This is clearly an upper limit. Further, under normal conditions of G5 emulsion-development, their estimate of the energy of a slow electron as 5 keV per grain is higher than the more usually accepted value of 3–4 keV per grain. (See Refs. 6 and 8). Zajac and Ross (Ref. 9) using NTA emulsion, found that for electron energies ≥ 30 keV the energy per developed grain corresponded to less than 3 keV.
The Auger-electron-emission rate has been determined a number of times by Eisenberg and collaborators. In the work of Eisenberg and Kessler (Ref. 7), quoted in Table I above, the authors observed that 52.9% of a random sample of K^- stars had one, or more than one, associated electron or blob. (The heavy-nucleus-emission frequency given for Eisenberg and Kessler's work in Table I is higher than the value that would be obtained by dividing 52.9% of electrons by 0.57, the fraction of heavy captures. The frequencies given in Table I, as previously mentioned, are calculated on the basis of the total number of electrons, and in a number of the 52.9% of stars there was more than one electron or blob emitted.)
From the work of Koch, Eisenberg, Nicolić, Winzeler, and Schneeberger (Ref. 10), the Auger rate from a random sample can be obtained by combining rates from a number of separate contributions as follows: 42% from multinucleon events, 34% from single nucleon events, and 22% from single nucleon events of the $\Sigma^{\pm}+\pi^{\mp}$ type. (The weights of the separate contributions were taken in the proportions found by these workers.) On the basis of this work, one concludes that only 36.3% of a random sample of K^- stars had one or more than one electron or blob. In this case, the electron-emission frequency is closer to, though still somewhat higher than, the values of the other workers (probably because of the inclusion of blobs).
The Auger-emission rate has been determined in yet another way by Eisenberg and collaborators (Ref. 11). In the work of Eisenberg and Kessler (Ref. 7), quoted in Table I, one finds from the experimental spectrum presented in their Fig. 9, that ~215 electrons or blobs with 10 or more grains were attributable to stopping K^- stars on the basis of 1000 events (278 actual events). As before, however, this number is higher than the yield that can be derived from earlier work of Eisenberg, Friedmann, Alexander, and Kessler (Ref. 11). From Tables IV and V of this earlier work, one can obtain by combining two-nucleon and single-nucleon K^- captures in the same ratio as before (i.e., from the work of Koch, Eisenberg, *et al.*) only 140 electrons having 10 or more grains in 1000 stopping K^- stars.
[g] From the data of Williams (Ref. 12) for ~20-keV electrons in aluminum, one concludes that the total electron range is ~1.35 times the straight-line distance travelled by the electron. Thus, if the range of a 20-keV electron is 3 μ, the average distance this electron will reach from the star center is only 2.2 μ. In the present work, we have required that the electron must have travelled at least 2 μ of projected range from the star, otherwise an electron track could not generally be distinguished from a blob. Thus it can readily be found that, because of dip and the variable direction of emission, the fraction of 20-keV electrons which would have been missed is $\sim(1-0.9/2.2)\sim 0.60$. Applying this correction, averaged over the various energy bins, gives the figure in parenthesis in Table I. The additional electrons in the bins, as obtained from this correction, are also given in the electron-emission spectrum of Fig. 1.

[4] E. B. Chesick and J. Schneps, Phys. Rev. **112**, 1810 (1958).
[5] C. Grote, I. Hauser, U. Kundt, U. Krecker, K. Lanius, K. Lewin, and H. W. Meier, Nuovo Cimento **14**, 532 (1959).
[6] M. Csejthey-Barth and J. Sacton, Université de Bruxelles, Institut de Physique: Services de Physique Nucléaire et de Metrologie Nucléaire, Bulletin No. 4, August 1962 (unpublished).
[7] Y. Eisenberg and D. Kessler, Phys. Rev. **130**, 2352 (1963).
[8] C. F. Powell, P. H. Fowler, and D. H. Perkins, *The Study of Elementary Particles by the Photographic Method* (Pergamon Press, Inc., New York, 1959), p. 169.
[9] B. Zajac and M. A. S. Ross, Nature **164**, 311 (1949).
[10] W. Koch, Y. Eisenberg, M. Nicolič, M. Scheenberger, and H. Winzeler, Helv. Phys. Acta **33**, 237 (1960).
[11] Y. Eisenberg, M. Friedmann, G. Alexander, and D. Kessler, Nuovo Cimento **22**, 1 (1961).
[12] E. J. Williams, Proc. Roy. Soc. (London) **A130**, 310 (1934).
[13] A. Pevsner, R. Strand, L. Madansky, and T. Toohig, Nuovo Cimento **19**, 409 (1961).
[14] G. T. Condo, Technical Report No. 36, Nonr 1834(05), Physics Department, University of Illinois, Urbana, Illinois, 1962 (unpublished).

quencies associated with certain types of K^- capture events, such as those emitting Σ hyperons only, $\Sigma^\pm+\pi^\mp$ (no star), $\Sigma^\pm+\pi^\mp+$star, etc. It was first reported by Koch *et al.*[10] that the Auger emission probability in nuclear emulsion is smaller for those K^--absorption events which produce charged $\Sigma\pi$ pairs only than for the average K^--capture star. Subsequently, this effect was noticed in this laboratory and also by Csejthey-Barth and Sacton.[6] Table II summarizes the Illinois and Brussels data on the electron emission from these special types of events. It is clearly seen that there is excellent agreement between the results from the two laboratories, especially when the emission probabilities are modified (as in columns 4 and 5) to take account of the different lower-energy cutoffs used in the two experiments. A possible explanation of the above results will be discussed in the next section.

TABLE II. Electron emission probabilities from charged hyperon producing events.

Event type	Fraction of stars emitting electrons of energies ≥20 keV (Illinois)	≥10 keV (Brussels)	Emission probabilities relative to probability for all captures col. 2 / 0.42	col. 3 / 0.65
Σ only (no star, no π)	0.55 (10/18)	0.78 (7/9)	~1.30	~1.20
Σ+star (no π)	0.27 (33/122)	0.33 (20/60)	0.64	0.51
$\Sigma^\pm+\pi^\mp$ (no star)	0.17 (21/124)	0.29 (20/70)	0.40	0.44
$\Sigma^\pm+\pi^\mp+$star	0.11 (4/36)	0.20 (2/10)	0.26	.31

III. ESTIMATE OF ELECTRON YIELD FROM K^--MESONIC PROCESSES

Possible mechanisms by which electrons are emitted following atomic capture of negatively charged K mesons will now be investigated. The mesonic atom is formed in a highly excited state and it then undergoes a rapid succession of electromagnetic transitions prior to nuclear capture. Recently, calculations have been made by Martin[2] and by Eisenberg and Kessler[7,15] on the Auger electron spectra arising from the mesonic cascades in the K^--mesonic atoms of Ag and Br. These Auger processes, as well as other disturbing background processes which have the appearance of Auger processes, will now be investigated.

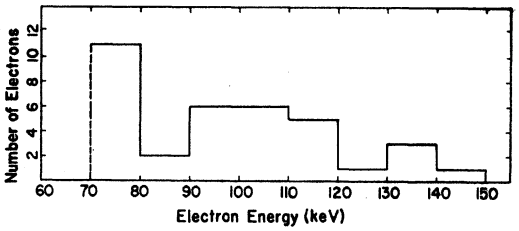

FIG. 2. Observed electron-energy spectrum (70–150 keV) for K^- mesonic atoms.

A. Radioactive and Isomeric Electronic Yield

It has generally been accepted that the Auger process has been responsible for practically all of the electron emission observed from mesonic atoms. It is true that a number of measurements of the background contribution due to chance juxtapositions of electron tracks with star vertices have been made, but these have generally been found insignificant. In the present experiment, such a test was made by examining ~5000 prong endings from K^- stars. An attempt was made to identify Σ^-p stars by the emission of electrons, but there was no observed contribution to the number of known Σ^--production events from proton endings.

It has often been stated that there is no contribution of electrons emitted from stars by radioactive fragments which must follow many disintegrations of heavy nuclei induced by meson absorption. This statement is based on the usual assumption that the beta-decay electrons from the radioactive fragments have energies which are too high to contribute to the normal Auger spectrum. However, this conclusion is largely erroneous because many low-energy isomeric transitions may be produced from the capturing Ag and Br nuclei. Preliminary, unpublished work (1958) by Elizabeth Johannson at the University of Illinois already gave indications of a substantial contribution of radioactive electrons produced from π-mesonic atoms. A similar investigation in the present stack of K^--meson interactions also provided evidence of some radioactive electron emission. In these experiments, the emission of low-energy electrons from a sample of neutron-induced stars, located in the same emulsion, was determined. The neutron stars were selected to have more or less the same appearance as the typical K^- stars. Twenty-two electrons (≥20 keV) were observed to emanate from the 260 neutron stars, thus corresponding to an electron-emission rate of approximately 8%. In four cases (not included in the 22) relatively fast electrons ≥100 keV were emitted from short recoil fragments of 0.8-, 1.1-, 3.7-, and 4.8-μ ranges.

[15] In the recent calculations of Eisenberg and Kessler, (Ref. 7) the effects of the binding energies of the atomic K-shell electrons have unfortunately been neglected. For example, Eisenberg and Kessler, in Fig. 8 of their paper, gave the following values for the energies of the K-shell Auger electrons from Ag: 23, 29, 38, 48, 68, and 95 keV. These energies are, in fact, the mesonic transition energies from the K-mesonic atom of Ag. Auger emission is possible for the last 5 of these values and the Auger electron kinetic energies, obtained by subtracting approximately 25 keV, which is the K-shell binding energy, are 4.3, 12.8, 24.9, 42.5, and 69.7 keV, respectively. The theoretical spectrum and intensity above 15 keV considered by Eisenberg and Kessler will, therefore, be much too large. The apparent agreement of their experimental results with their theoretical electron spectrum very probably derives from the features of their experiment already mentioned in footnote (f) of Table I, viz., (i) the inclusion of all blobs as electrons and (ii) the increase of electron energies above the more commonly accepted range-energy values.

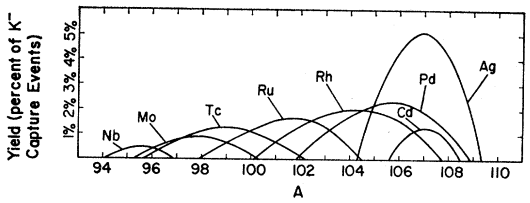

FIG. 3. Estimated nuclide yields from K^--absorption reactions on Ag. The yields are given for captures in a natural mixture of Ag^{107} and Ag^{109} isotopes of silver and as a percentage of the total number of K-meson capture events in Ag and Br assuming a Fermi-Teller Z law.

It seems probable that electron emission of this nature could also be induced by meson absorption at rest, except, in this case, owing to lack of center-of-mass motion, the recoiling fragments might be indistinguishable from the star center.

A test for radioactive electron emission using neutron stars, apart from the inherent defect of requiring relatively high-energy neutrons in order to produce the same energy stars as arise from meson absorption, is not satisfactory because different radioactive species will be produced by different agencies. An attempt to evaluate the yield of specific radioactive products has therefore been made using experimental information on K^- stars together with known nuclear data.

The experimental information on K^- stars produced in G5 emulsion has been given by the K^- collaboration group.[16] They list the number of visible prongs and their frequencies for the following types of events: $\Sigma^\pm+\pi^\mp$, π+double star, π (no Σ), Σ (no π), no π no Σ, and stable prongs only. They also found that the π^-/π^+ ratio was approximately 4, and that the Σ^+/Σ^- ratio was 4. If to this information is added the generally accepted figure that on the average 2 neutrons are evaporated for every one slow proton,[17] then the yield of nuclear fragments of all Z from 48 to 39 and A from 108 to 95 for Ag, and all Z from 37 to 27 and all A from 80 to 62 for Br, can be evaluated. Such yields estimated in the above fashion are given in the curves of Figs. 3 and 4.

In estimating the electron contributions possible for a particular Z and A nuclear fragment, a number of points must be considered. The most essential data, of course, are the electron spectra of the nuclide. Generally, however, for the region of the Z and A produced, the intensities of electrons in the 20–100-keV range are well known. It is generally true that the contributions from continuous beta-ray spectra are relatively small. The main contributions are found to arise from isomeric transitions, for example, Ag^{109m}, Ag^{107m}, Rh^{104m}, Rh^{103m}, Kr^{79m}, Br^{80m}, Br^{78m}, Se^{79m}, Se^{77m}; however, in some cases there are significant small contributions from low-energy conversion electrons, such as 6.7-h E. C. Cd^{107}, 6-min E. C. Br^{78}, etc. (The feasibility of studying the complex electron spectra of Pd^{109}, Ag^{109m}, Se^{81m}, and Se^{81} by using G5 nuclear emulsions has recently been shown by Cartacci, Dagliana, and Tocci.[18]) One of the problems is to decide on the production intensity of an isomeric nuclide. Lacking definite evidence in the case of K^- absorption products, it has been assumed that the relative isomeric and ground-state yields for a particular A and Z are in the ratio of their spin statistical weights. A further point that must also be taken into account in considering the emission of detectable electrons is the lifetime of the radioactive nuclide in relation to the time between exposure of the emulsion and its development. On the basis of all the above assumptions, and also the highly probable eventuality that all of the radioactively emitted electrons arise from K^- absorptions in Ag and Br, it is found that approximately 27% of the K^- stars in AgBr should emit electrons in the energy range (20–100 keV) of a radioactive nature. The spectrum of such electrons is shown in Fig. 5.

Another strong indication that radioactive electrons contribute to the electron emission observed in K^--mesonic atoms is given by the hitherto unexplained results on the low emission of Σ-producing events. These results were summarized in Table II. The explanation of this effect is probably to be found in the low contribution of radioactive background electrons in K^--capture stars associated with Σ emission. This is not altogether unexpected, for the internal absorption of a Σ will generally produce quite different end-product nuclides.

A very good check on this explanation can be made by considering the particular cases of $\Sigma^\pm+\pi^\mp$+star. These cases lead to precisely known atomic number products and the star also allows the number of captures in light and heavy nuclei to be broken apart. Reference to Table II shows that there were 36 cases of $\Sigma^\pm+\pi^\mp$+star, of which there were 25 cases with 3 prong, 10 cases with

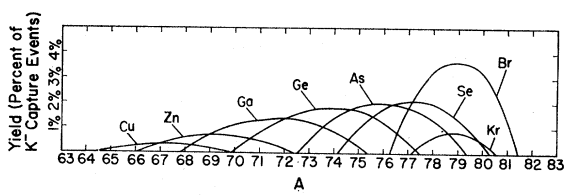

FIG. 4. Estimated nuclide yields from K^--absorption reactions on Br. The yields are given for captures in a natural mixture of Br^{79} and Br^{80} isotopes of bromine and as a percentage of the total number of K-meson capture events in Ag and Br assuming a Fermi-Teller Z law.

[16] B. Bhowmik, D. Evans, D. Falla, F. Hassan, A. A. Kamal, K. K. Nagpaul, D. J. Prowse, M. René, G. Alexander, R. H. W. Johnson, C. O'Ceallaigh, D. Keefe, E. H. S. Burhop, D. H. Davis, R. C. Kumar, W. B. Lasich, M. A. Shaukat, F. R. Stannard, G. Bacchella, A. Bonetti, C. Dilworth, G. Occhialini, L. Scarsi, M. Grilli, L. Guerriero, L. von Lindern, M. Merlin, and A. Salandin, Nuovo Cimento **13**, 690 (1959).

[17] K. J. LeCouteur, Proc. Phys. Soc. (London) **A63**, 259 (1950); P. Morrison in *Experimental Nuclear Physics*, edited by E. Segrè (John Wiley & Sons, Inc., New York, 1953), Vol. II, p. 177.

[18] A. M. Cartacci, M. G. Dagliana, and L. Tocci, Nuovo Cimento Suppl. **21**, 21 (1961).

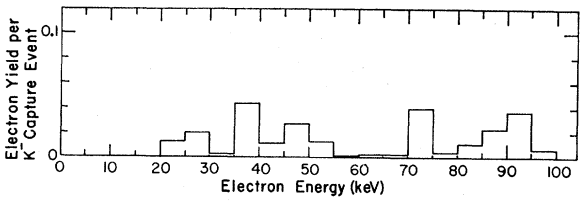

FIG. 5. Estimated energy spectrum of electrons from radioactive background arising from K^--meson absorption in AgBr.

4 prongs, and 1 case with 5 prongs. There were the following numbers with short prongs: 15 cases with 3 prong, 6 cases with 4 prongs, and 1 case with 5 prongs, thus indicating that 22 cases out of 36 could be identified as light nucleus captures. Only 4 cases of electron emission were observed, all cases associated with captures in heavy nuclei. There was, therefore, an electron emission rate of 4 in 14 cases, or 28.5%. It is probable, however, that not all of this rate was due to Auger electron emission.

The amount of radioactive-electron contribution from the $\Sigma^{\pm}+\pi^{\mp}+$star type of events has been estimated by reference to the scheme of reactions given in Appendix IV. In this type of event there is a limited number of reactions in Ag and Br. The percentage figures in front of the four main reactions are determined by the assumption of a Z capture law and the nuclear abundances of Ag^{109}, Ag^{107}, Br^{81}, and Br^{79}. The percentage figures following each fragmentary reaction are determined from the observed numbers of 3-, 4-, and 5-prong reactions associated with the $\Sigma^{\pm}+\pi^{\mp}+$star type of event and the relative neutron evaporation theory rates which are consistent with the curves of Figs. 3 and 4 already given. From a knowledge of the electron spectra and lifetimes of the nuclear fragments, the intensity of radioactive electron emission can then be found. In these particular events, in which $\Sigma^{\pm}+\pi^{\mp}+$star are produced, it was calculated that radioactive electrons should be associated with only approximately 6% of the events. Thus, it is concluded that the true Auger-emission rate is (28.5-6) or approximately 22%, a value which is in excellent agreement with the rate previously derived from all classes of K^--capture events.

B. Auger Electron Spectrum from K-Mesonic Ag and Br Atoms

In this section the computed spectra of the Auger electrons from K^- capture in AgBr are summarized. Since several calculations of Auger cascades have already been described in detail,[19] the method used in the present analysis will be only briefly sketched. The present computation was started in the $n=16$ mesonic level, commencing in each of the angular momentum substates in turn. Thus, the Auger spectrum resulting from any particular initial distribution at the $n=16$ level can be predicted. This level was taken as the starting point because very few Auger electrons of $\gtrsim 20$ keV are to be expected from transitions with $n \geq 16$. Further, mesons from the $n=16$ level will make several transitions prior to ejecting K-shell Auger electrons, which constitute the major portion of the observable spectrum.

Only dipole transitions have been assumed to occur (quadrupole transitions are considered briefly in Sec. V.) All possible such transitions, including radiative and Auger transitions involving K-, L-, and M-shell electrons, have been calculated with the aid of the University of Illinois, IBM-7090 computer. The formulas used for calculating these rates are given in Appendix II. The computation was limited, however, to transition probabilities which were larger than 0.5% of the total transition probability from any state. This was necessary in order to keep the amount of computation within reasonable bounds. The cascade of a meson from each substate of the $n=16$ level was followed separately in Ag and Br until nuclear capture occurred, which was assumed whenever the meson reached a state of $l \leq 3$. The resulting Auger spectrum, however, is not dependent on this assumption. Consolidation of the results for Ag and Br into a heavy-nucleus spectrum was effected by invoking the Fermi-Teller Z law,[20] whereby captures in Ag and Br are taken in the ratio of their atomic numbers, 47 and 35.

The results of the cascade calculations are shown in Figs. 6, 7, and 8. The spectrum shown in Fig. 6 is for an initial distribution of 100% mesonic atoms in state $n=16$, $l=15$, such that all transitions occur via the circular orbits. The total electron yield (20–100 keV)

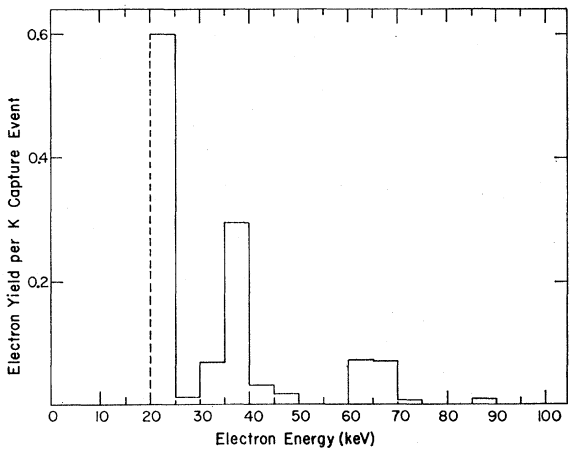

FIG. 6. Theoretical Auger electron-energy spectrum. The initial population for this spectrum was 100% of K^- mesonic atoms in the $n=16$, $l=15$ state (circular orbit case).

[19] E. H. S. Burhop, Proc. Roy. Soc. (London) **A148**, 272 (1935); G. R. Burbidge and A. H. deBorde, Phys. Rev. **89**, 189 (1953); A. H. deBorde, Proc. Phys. Soc. (London) **A67**, 57 (1954); M. Demeur, Nucl. Phys. **1**, 516 (1956).

[20] E. Fermi and E. Teller, Phys. Rev. **72**, 399 (1947).

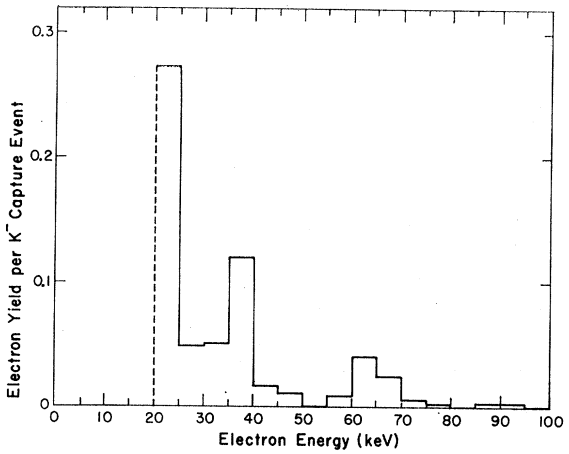

FIG. 7. Theoretical Auger electron energy spectrum. The initial population for this spectrum was 100% of K^--mesonic atoms in statistically distributed states according to a $(2l+1)$ law in the $n=16$ level.

per K^--capture event in this case is 1.19. The large yields in the 20-25- and 35–40-keV bins are characteristic features of the circular orbit transitions. The spectrum shown in Fig. 7 is for a "$2l+1$" statistical distribution in the initial $n=16$ state. The total electron yield (20–100 keV) in this case is 0.61 electrons per K^--capture event. This spectrum shows many of the same characteristic peaks as in the purely circular orbit transitions. Figure 8 shows the Auger distributions for two different starting points: one the $l=8$ substate of $n=16$, the other the $l=7$ substate of $n=16$. The electron yield between 20 and 100 keV is only 0.29 per K^--capture event in the case of $l=8$, $n=16$.

C. Comparison of Experimental Results with Theoretical Prediction

There are two grounds on which the experimental results can be compared with theory, namely, on the basis of the total electron yield or on the shape of the electron-energy distribution. First, however, the observed electron yield must be corrected for the background of electrons emitted in radioactive decays. The observed yield and the expected radioactive background

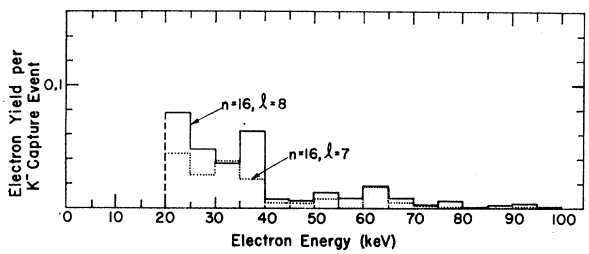

FIG. 8. Theoretical Auger electron energy spectra. Two spectra are given for different initial distributions of the K^--mesonic atoms: (1) 100% in the $l=8$, $n=16$ state, and (2) 100% in the $l=7$, $n=16$ state.

are plotted from 20 to 70 keV in Fig. 9. (The observed yields in the 20–30- and 30–40-keV bins have been increased by 37 and 4%, respectively, in order to correct for the loss of electrons undetected because of the geometrical factor mentioned in footnote g of Table I.)

Comparison of Fig. 2 with Fig. 5 shows that above 70 keV, the expected radioactive background is a few percent higher than the observed spectrum. Although the yields are probably the same within the significance of the experiment and analysis in this 70–100-keV region, there could nevertheless be possible systematic factors which are responsible for the difference. The first possibility is that the radioactive yield is too high because the production of a particular activity has been estimated incorrectly from its spin statistical weight. Cases of isomers whose isomeric ratios in neutron-capture production are not given by their spin statistical weights are known. The peaks in the 70–75- and 90–95-keV bins of Fig. 5 are largely contributed by a single isomeric activity, but in this case, since there is only

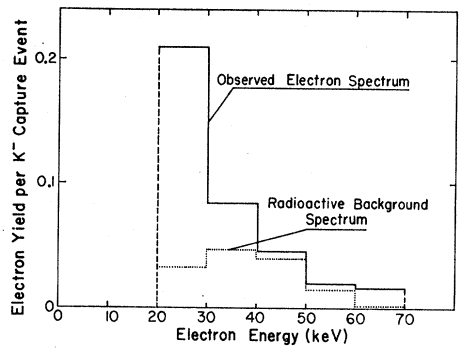

FIG. 9. Comparison of observed Auger and expected radioactive electron spectra from K^--capture events in AgBr.

one active level (the isomeric activity), no experimental information is available on the isomeric ratio. The second possibility is that the efficiency of electron detectability falls off in the region near 100 keV. Although it is difficult to assess detection efficiency, it is clear that a 100-keV electron track with 48 μ range will have a higher probability for being scattered and not being detected than a 50-keV electron with only 15-μ range. Moreover, the grain density at the start of a 100-keV electron track is somewhat less than that of a 50-keV electron. In view of these factors, therefore, it seems preferable to limit a comparison between the two spectra below 70 keV. The final Auger yield, then, obtained by subtracting the radioactive background from the observed spectrum in the 20–70-keV range is $\sim$24%.

The theoretical electron distributions computed in Sec. III(B) are compared with the true experimental Auger distribution in Fig. 10. All distributions shown are normalized to the same total percentage of 24. Although there does not appear to be much to choose

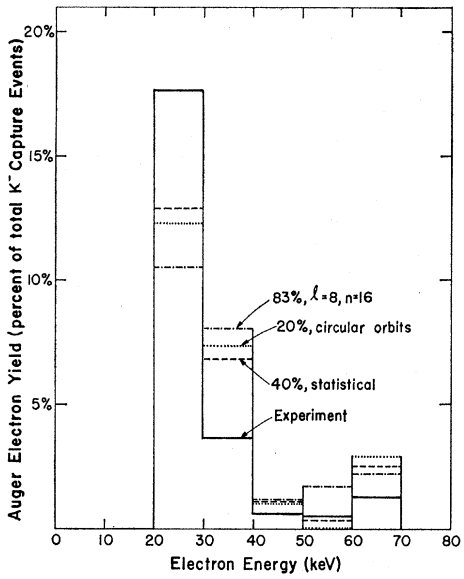

FIG. 10. Comparison of experimental and theoretical Auger electron spectra.

between any of the theoretical distributions in regard to their agreement with experiment, the one which is 40% of the statistical distribution probably agrees best. In the next section it will be shown that there are grounds for believing that the total number of K^--capture events giving rise to observable Auger electrons might be depleted to approximately 40%. Probably the poorest agreement as far as the distribution shape is concerned is the case of the single $l=8$ substate distribution. This value of l (and $n=16$) is the lowest for which the total theoretical electron yield exceeds the 24% observed yield. [The yields for $l=7$ and $l=6$ (and $n=16$) are only approximately 73 and 36% of the experimental yield.] It will also be seen in the next section that a single initial state distribution in the $n=16$ level with l as high as 8 is rather improbable.

IV. DISCUSSION AND POSSIBLE INTERPRETATIONS OF ELECTRON YIELDS FROM MESONIC ATOMS

From the comparison between the observed and theoretical electron distributions and intensities made in Sec. III, it is clear that the population of K^- mesons reaching the $n=16$ state is either considerably reduced or modified from that conventionally assumed. In between capture from the free state and in cascading to the $n=16$ state, many K mesons must either be absorbed or evade the region in which the observable Auger electrons are emitted. Because of the complicated nature of both the K meson and electron wave functions, however, the capturing and cascading processes of K^- mesons in solid materials have not yet been described. For μ-meson capture in solids, the process has been investigated in a quantum statistical manner by Fermi and Teller,[20] but only in a semiqualitative way for insulating materials. Using their arguments for K mesons, one may estimate that a K meson will cascade into the region of the K-electron shell radius of either Ag or Br in crystalline AgBr in times of the order of a few 10^{-13} sec.

A complete description of the K^--meson capture and cascade must necessarily include many solid-state effects. Initially, moderation of the K meson will probably occur via excitation of the valence-band atomic electrons either to the conduction bands of the crystalline AgBr or to the continuum. It is estimated that these Auger-type transitions occur in times of the order of 10^{-15} sec and quicker, and consequently it is expected that they will dominate over those collective processes, such as phonon transitions, which transfer energy to the crystal as a whole.

After excitation or ejection of a few electrons, the K meson will become localized in the region about one of the lattice centers. Again, it is clearly a very poor approximation to regard the K-meson wave function at this stage as approaching, even remotely, hydrogenic. Probably a reasonable approximation, however, to the wave function at the stage when the K meson does become significantly bound to a single atom, is the WKB approximation based on the accurately known screened field of the atom derived from a Hartree-Fock potential.[21] No calculations of the matrix elements using WKB wave functions were attempted in the present paper, but estimates of the K^--meson energy-level values in the region of the K- through N-electron shells, based on the Hartree-Fock potentials of Ag^+ were used.

It is found that the Auger mechanism, in general, favors mesonic transitions that are accompanied by the smallest possible excitation of the atomic electron, assuming uniform density of the available electron states. Thus the form of the mesonic de-excitation will be further complicated because, due to the fast rate of the Auger ionization process, the host atom of a K^- meson will probably lose many of its outer electrons during this rapid sequence of low-energy mesonic transitions. If this multiple ionization occurs on a halide ion of the AgBr crystal, the situation is similar to that considered in the theory of defect formation[22–25] in ionic crystals. For example, the Varley mechanism for x-ray production of lattice defects is considered to occur following double ionization of a halogen ion. The doubly ionized halogen ion having a net positive charge is thus repelled, by the surrounding electrostatic field, to an interstitial site where it is considered to form a halogen molecule with a neighboring ion. The possibility of such a process and the various intermediate steps are some-

[21] B. J. Worsley, Proc. Roy. Soc. (London) **A247**, 390 (1958).
[22] J. H. O. Varley, Nature **174**, 886 (1954) and J. Nucl. Energy **1**, 130 (1954); C. C. Klick, Phys. Rev. **120**, 760 (1960); R. E. Howard, S. Vosko, and R. Smoluchowski, *ibid.* **122**, 1406 (1961); R. E. Howard and R. Smoluchowski, *ibid.* **116**, 314 (1959).
[23] F. E. Williams, Phys. Rev. **126**, 70 (1962).
[24] D. L. Dexter, Phys. Rev. **118**, 934 (1960).
[25] J. H. O. Varley, Phys. Chem. Solids **23**, 985 (1962).

what controversial and have been discussed at length by the above authors. It would appear that the critical factor is the time of formation τ_M of the halogen molecule in comparison with the time τ_H for the separation of the two positive holes, i.e., τ_H is the time for the halogen ion to recover one electron. Estimates of these times are: $\tau_M \sim 10^{-13}$ sec and $\tau_H \sim 3\times 10^{-14}$ sec obtained by Williams[23] for KCl in the tight binding approximation, $\tau_H \sim 10^{-15}$ sec proposed by Dexter[24] on the basis of the band model, and $\tau_H \sim 10^{-12}$ sec employed by Varley[25] for KCl, and for which the time is dependent on the width of the valence band. The main difference between x-ray ionization and mesonic-capture ionization, via Auger emission, is that in the latter the ionization is a continuing process as the meson cascades further in toward the nucleus. In the mesonic-capture case, as the degree of ionization of the ion increases, the times τ_M and τ_H will quickly diminish until the frequency of electron replenishment τ_H^{-1} equals the frequency for Auger emission, i.e., $\sim 10^{15}$ sec^{-1}. When this equilibrium is reached, we estimate that the net charge of the mesonic atom will be of the order of $+5$. However, as the cascade continues, the neighboring lattice ions will also become multiply ionized. One must therefore conclude that there is a very strong probability that not only a Br mesonic ion, but also a Ag mesonic ion, will be displaced from its lattice site when it captures a K^- meson.

In the light of the foregoing discussion of the capture process in solid material, two mechanisms have been considered for explaining how the Auger yield is found to be less than the theoretically expected value. The first is to accept that the initial population of angular momentum states of a high n value (principal quantum number) are peaked, in a way discussed by Baker[26] and Martin,[2] at an l value (angular momentum quantum number) of approximately $n/3$. By following the transitions in a semiquantitative way, it will appear plausible that the majority of K^- mesons can be absorbed on the nuclear periphery at $n>30$ and thus evade transitions through the region of $6<n<11$ and $l \lesssim n-1$, in which the main contributions to the observed Auger spectrum arise. The second alternative explanation is to accept that the displacement of the mesonic atom causes a Stark effect which disturbs the level population in the region of $n=70$ so as to cause nuclear absorption of a large fraction of K mesons. The remaining K mesons then proceed in the expected fashion to lower n regions and achieve an approximately statistical distribution at $n=16$, thus leading to a normal Auger electron distribution of reduced intensity.

A. Peripheral Nuclear Absorption and the Absence of Auger Electrons

Both Baker[26] for hydrogen and Martin[2] for Ag and Br have shown that the atomic capture of K^- mesons occurs to highly excited mesonic states. The value of the principal quantum number n of the capture state corresponds to the meson being located in the region of the orbit of the electron ejected by the capture mechanism; the population distribution of the angular momentum substates is strongly peaked in the region $l \sim n/3$ to $n/2$. This last result requires atomic captures at mesonic kinetic energies of at least 50 eV for Ag and Br. Although both of these calculations were for free atoms, it is not unlikely that similar results would be obtained for K^--meson capture in an ionic crystal.

As a starting point in the cascade calculation, the $n=95$ level of Ag in a AgBr crystal at a binding energy of approximately 500 eV (as shown by a WKB approximation calculation in Appendix III) was chosen. This value of n was selected because the K meson is well within the $4d$-electron-shell radius and therefore the use of screened hydrogenic wave functions should provide an increasingly reliable estimate of transition rates as the meson cascades nearer the nucleus. Furthermore, with this small binding energy, the angular momentum distribution should still be peaked around $l \sim 40$.

Computing the dipole mesonic transition rates for such states in Ag, according to the assumptions outlined in Appendix II, it is found that the $\delta n=-1$, $\delta l=-1$ Auger transition is dominant. However, in this region of the cascade both the $\delta n=0$, $\delta l=-1$ and the $\delta n=-1$, $\delta l=0$ Auger transitions must also be considered. The first of these transitions is possible due to the lack of degeneracy of the angular momentum substates of a highly excited mesonic level, investigated in Appendix III. For a pure AgBr crystal the valence electrons require only ~ 2.5 eV to be excited into the conduction band.[27] Allowing for the increase of the minimum electron-excitation energy in the multiply ionized Ag we find that the $\delta n=0$, $\delta l=-1$ transitions are possible for mesons occupying angular momentum substates $l \gtrsim n/2$ and compete strongly with the $\delta n=-1$, $\delta l=-1$ transition. The $\delta n=-1$, $\delta l=0$ Auger transition is negligible in comparison to the dipole transitions if the mesonic orbit is well within the mean radius of the state from which the electron is ejected, a condition probably well satisfied in the region being considered.

Thus, by means of a sequence of dipole transitions, the meson de-excites from its initial state into the region $n \sim 60$, but now the population of angular momentum substates is peaked around $l \sim 8$. In this "intermediate" region two new effects should be considered: one is the peripheral nuclear absorption of K mesons populating the ng and nf states, as pointed out by Jones[28] and others[29]; the other effect is the possibility that, for small l, purely radiative transitions of large δn start to compete with Auger transitions. Table III, however,

[26] G. A. Baker, Jr., Phys. Rev. **117**, 1130 (1960).

[27] F. C. Brown, J. Phys. Chem. **66**, 2368 (1962).

[28] P. B. Jones, Phil. Mag. **3**, 33 (1958).

[29] D. H. Wilkinson, Phil. Mag. **4**, 215 (1959); J. R. Rook, Nucl. Phys. **39**, 479 (1962).

TABLE III. The dominant electromagnetic transitions,[a] $(n_1,l_1) \rightarrow (n_2,l_2)$, and the branching ratios from various angular momentum substates of:
(i) the $n_1=50$ mesonic level of Ag

$l_1=2$[b] Transition $\rightarrow$ (n_2,l_2)	% Probability	$l_1=3$[b] Transition $\rightarrow$ (n_2,l_2)	% Probability	$l_1=8$ Transition $\rightarrow$ (n_2,l_2)	% Probability	$l_1=20$ Transition $\rightarrow$ (n_2,l_2)	% Probability	$l_1=40$ Transition $\rightarrow$ (n_2,l_2)	% Probability
Rad. $\rightarrow$ (2,1)	21	A(M) $\rightarrow$ (48,2)	27	A(M) $\rightarrow$ (48,7)	44	A(M) $\rightarrow$ (48,19)	57	A(M) $\rightarrow$ (48,39)	86
A(M) $\rightarrow$ (48,3)	21	A(M) $\rightarrow$ (48,4)	23	A(M) $\rightarrow$ (48,9)	16	A(M) $\rightarrow$ (47,19)	15	A(M) $\rightarrow$ (47,39)	12
A(M) $\rightarrow$ (48,1)	19	Rad. $\rightarrow$ (3,2)	8	A(M) $\rightarrow$ (47,7)	12	A(M) $\rightarrow$ (46,19)	6		
Rad. $\rightarrow$ (3,1)	8	A(M) $\rightarrow$ (47,2)	7	A(L) $\rightarrow$ (43,7)	5				
				A(M) $\rightarrow$ (46,7)	5				

(ii) the $n_1=20$ mesonic level of Ag

$l_1=2$[b] Transition[a] $\rightarrow$ (n_2,l_2)	% Probability	$l_1=5$ Transition $\rightarrow$ (n_2,l_2)	% Probability	$l_1=10$ Transition $\rightarrow$ (n_2,l_2)	% Probability	$l_1=15$ Transition $\rightarrow$ (n_2,l_2)	% Probability
Rad. $\rightarrow$ (2,1)	50	A(L) $\rightarrow$ (19,4)	22	A(L) $\rightarrow$ (19,9)	50	A(L) $\rightarrow$ (19,14)	71
Rad. $\rightarrow$ (3,1)	18	Rad. $\rightarrow$ (6,4)	9	A(K) $\rightarrow$ (17,9)	11	A(M) $\rightarrow$ (19,14)	9
Rad. $\rightarrow$ (4,1)	9	Rad. $\rightarrow$ (5,4)	8	A(M) $\rightarrow$ (19,9)	6	A(K) $\rightarrow$ (17,14)	6
		Rad. $\rightarrow$ (7,4)	8				

[a] Rad. and A(I) abbreviate radiative and Auger transition with the ejection of an I-shell electron, respectively.
[b] Note that in the $l=2$ and $l=3$ states the nuclear capture of the mesons will dominate the above transition processes.

shows this last effect is not significant; the large δn radiative jumps compete only from the $l \leq 3$ substate of the $n=50$ mesonic level. Thus, assuming that the population is peaked at $l \sim 8$ and that all the contributing cascade processes have been included, there is therefore no possibility of populating mesonic states in the region $n \sim 10$, $l > 2n/3$ of the cascade. Remembering that mesonic transitions in this region of the cascade are responsible for almost entirely all the observable Auger electrons, we expect at the very most an Auger yield of 5%.

In the above description of the mesonic cascade it has been assumed that the initial population of angular momentum substates is peaked at $l \sim n/3$ and that the transition rates for the very highly excited mesonic states are reliably estimated using screened hydrogenic wave functions. However, the resulting absence of Auger electrons is not very sensitive to these assumptions. First, because any population of angular momentum substates $l > n/2$ would soon peak in the region $l \sim n/2$ due to the dominance of the $\delta n=0$, $\delta l=-1$ Auger transition for high n and l; and second, because the use of screened hydrogenic functions certainly becomes an applicable approximation when the K^- meson is inside the M-shell electrons.

B. Possible Explanation of the Observed Auger Yield by Stark Mixing in Highly Excited Levels

An alternative mechanism for bringing about nuclear capture in high n states ~ 70 is seen in the Stark mixing of neighboring angular momentum substates. The manner in which the Stark effect is believed to occur is as follows. It has been pointed out that an ion capturing a K^- meson will undoubtedly be displaced from its site in the crystal lattice. An estimate of the electric field on the multiply charged ion by the surrounding and disturbed AgBr lattice is readily shown to be $\sim e/R^2$ where $R \sim 1$ Å. However, critical to the occurrence of the Stark mechanism is the time of formation of this field.

In the theory of defect formation in ionic crystals we have seen that a doubly ionized halide ion, or alternatively two adjacent singly ionized halogen ions, probably experience forces that would cause displacement of the halogen from its lattice site in a time the order of 10^{-13} sec.[23] It was also noted that mesonic capture causes multiple ionization of the host atom in a time of the order of 10^{-15} sec, and due to the recovery of its atomic electrons will be continually ionizing neighboring ions in times τ_H of this order or quicker. However, in the case of mesonic ionization, not only do we expect τ_H to be shorter than in the theory of defect formation, but τ_M also. Indeed, this turns out to be consistent, for, if we consider $\tau_M \sim 10^{-14}$ sec we find, due to the electric field mentioned above, a movement of the lattice ion by a considerable fraction of its lattice spacing. It thus appears very probable that, owing to the considerable disturbance of the lattice within its neighborhood, the mesonic atom will experience a very strong electric field in a time the order of 10^{-14} sec following capture, varying in both strength and direction in times of this order. It is very probable that such a field may be responsible for considerable Stark mixing of the degenerate mesonic states.

The range of n of the K-mesonic atom in which the Stark effect will be important is probably $70 < n < 100$. The upper limit of n values will be determined by the time required for the generation of a multiply charged ion and also by the onset of its displacement from its

initial lattice site. Both of these requirements will probably be met by the time the K-meson orbits are localized in the region of the M-electron shell, i.e., when n for the mesonic atom is ~ 100. The lower limit of n values will be reached when the M- and L-shell electrons begin to shield the K meson from the externally produced Stark field. This will probably occur when the K-meson orbits lie within the region of the L-electron shell, or n for the mesonic atom is $\lesssim 70$.

The rate of Stark "transitions" may be estimated from the matrix element for mixing adjacent degenerate angular momentum l substates of a given n level. In the sense of the simplest model of the electric field, if the Stark splitting is produced by a charge pe at a distance R, then the Stark mixing rate is given by

$$\Gamma_{l\to l-1}\sim\frac{n(n^2-l^2)^{1/2}}{[R(\text{Å})]^2}\frac{p}{Z_{\text{eff}}}\times 10^{13}(\text{sec}^{-1}),$$

where Z_{eff} is the effective charge experienced by the K^- meson. Thus, if p is assumed to be $+1$ and R is 1 Å, as appears consistent with the description of the lattice disturbance, the transition time for $n=90$ and low l values will be $\sim 4\times 10^{-16}$ sec, and for $n=70$ and low l values will be $\sim 8\times 10^{-16}$ sec. Now, although the Auger transition times are somewhat slower in the $70<n<90$ region than in the initial phase of the K meson's capture, they will still be of the order of 10^{-14} sec and therefore, if the angular momentum states are degenerate, there will be of the order of 20 Stark transitions per Auger jump. (It should be noticed that this Stark mixing is probably stronger in the Br atom than the Ag, for two reasons: first, there will be fewer electrons in the Br ion shielding the mesonic orbits from the Stark field, and second, the neighboring lattice ions to a Br mesonic atom are ordinarily positively charged; thus the doubly ionized Br ion immediately feels the repulsive force of the disturbed surrounding field, whereas for the Ag ion, it first has to rob electrons from the neighboring ions in order to establish its field.)

In order to determine the extent of the level degeneracy in this region of n, it is necessary to consider three effects: (i) the broadening of levels assuming the above Stark effect, (ii) the splitting between l levels of the same n which arises from different penetrations of the K-mesonic orbits into the electron-screened nuclear field, and (iii) the level shift and broadening in low l states arising from the short-range K-meson nuclear interaction. For an electric field e/R^2 with $R\sim 1$ Å, the energy available for Stark splitting of the angular momentum substates of the $n=80$ level, for example, is ~ 10 eV. The splitting caused by the second effect has been investigated in some detail using the WKB approximation mentioned earlier in this section and is described further in Appendix III. For instance, it is seen that in the region of the level $n\sim 80$ the degeneracy of substates is such for $l\lesssim 15$ as to offer no impedance to the Stark mixing; however, for higher angular momentum substates, there will be an increasing tendency to prohibit these transitions, and for $l>n/2$ substates they are likely to be almost absent. There will thus be a strong tendency to populate the low angular momentum substates in a "$2l+1$" or statistical distribution. Also, as can be seen from part A of this section, the population of the higher l substates is continually being depleted by the rapid sequence of $\delta l=-1$ Auger transitions. Consequently, it is reasonable to assume that the population distribution of substates of such highly excited levels approaches a "$2l+1$" distribution up to $l\sim n/3$ and falls off rapidly for higher l substates.

The third effect mentioned in the previous paragraph is also discussed in Appendix III. In the region of $n\sim 80$ it is expected that the rate for nuclear capture will dominate all other transitions for mesons populating ns, np and nd substates and compete strongly for mesons in the nf state. Thus, a succession of dipole transitions will result in the nuclear absorption taking place from f states and, provided the dipole transition time is sufficiently short (less than 10^{-15} sec), also an appreciable fraction of absorption from d states.

In order to estimate the fraction of nuclear captures *per* Auger jump between highly excited mesonic states, it is necessary to determine the fraction of the population of a mesonic level reaching the nf state via the Stark mixing that occurs between Auger transitions. Using the level-population distribution obtained above and assuming mixing between the m substates (corresponding to the $2l+1$ orientations of angular momentum) it is estimated that an average of $\sim 2\%$ of the mesons are captured for each of the ~ 20 Auger jumps taking place in the region of the cascade where the Stark mechanism is important. The relative fraction of these mesons captured from the d and f states depends on the ratio of the Stark-mixing rate to the nuclear-capture rate from the f state. This latter rate in the $80f$-state is calculated to be 5×10^{15} sec^{-1}, and is increased to 2×10^{16} sec^{-1} if the effect of a 20-MeV attractive K^--meson nuclear potential is included.

According to the Stark-effect description of the cascade, the majority of mesons surviving in the $n\sim 60$ level should be distributed "statistically" in the l substates up to $l\sim 25$. Continued nuclear absorption will occur in the remainder of the cascade, from the f states at first but with increasing amounts of g-state capture for those mesons reaching low-lying mesonic levels. Due to increasing competition from those transitions with $\delta n<-1$, we estimate it is likely that approximately 20–40% of the original mesons will reach the $n\sim 16$ level and these will populate the substates in a distribution comparable to a statistical one. This result appears to be consistent with the experimental observations, as was shown in Sec. III. It should be emphasized that this fraction of mesons survives and reaches the region of the cascade giving rise to observable Auger electrons,

only because Stark mixing in the highly excited states removes the dominance of $\delta l=-1$ Auger transitions.

V. APPLICATION TO THE MULTINUCLEON CAPTURE OF K^- MESONS

The experimental fact[30] that a substantial fraction of K^- mesons undergoes nuclear absorption with a pair (or more) of nucleons, instead of with a single nucleon, has been the source of considerable discussion.[29,31] Mesonic-cascade calculations, starting from the region of the electronic K shell and based on the transition rates for the conventional cascade processes, predict almost exclusive nuclear absorption of the meson from the nucleus periphery, e.g., for Ag and Br mainly from the $5g$-mesonic state. It has been difficult to resolve these questions of multinucleon captures without invoking some sort of clustering of nucleons in the peripheral region (e.g., Wilkinson's "spikey" nucleus model of α-particle clusters on the nuclear surface). From the discussion in Sec. IV, however, it is now seen that a considerable fraction of nuclear absorptions of K^- mesons occurs from highly excited meson states. Using a simplified model of the nucleus, the radial dependence of capture of a meson in a state (n,l) may be found from the mesonic radial wave function $R_{nl}(r)$ and the nucleon density distribution $\rho(r)$. For example, for a zero-range meson-nucleon interaction, the radial distribution of single-nucleon K^- capture is $\sim\rho(r)r^2|R_{nl}(r)|^2$ and of two-nucleon K^- absorption (assuming no particular nucleon correlations) is $\sim\rho^2(r)r^2|R_{nl}(r)|^2$. For a given l, the form of $R_{nl}(r)$ that overlaps with the nuclear density is essentially independent of n and, consequently, the radial probability distribution for capture is largely independent of excitation of the mesonic level. On the other hand, the nuclear-capture rate for fixed l decreases with increasing n (approximately as $1/n^3$) due to the normalization factor of $R_{n,l}$. Thus, for highly excited states ($n\sim80$), without invoking any new mechanism, nuclear capture may still be expected from lower l states than is usually assumed. Indeed, one finds that the K^- meson reaches an $l=3$ state before the nuclear-capture rate favorably competes with the dipole transition rates and, further, if the Stark mechanism is invoked (as in the previous section), an appreciable fraction of captures may occur from the $l=2$ substates of highly excited mesonic levels. In contrast to nuclear absorptions from $l\geq3$ states, it is found that the majority of mesonic captures from d states occur in regions of high nucleon density. For instance, using the simple model above, computation of R_{nd} for a 20-MeV attractive K^- nuclear potential shows that $\sim80\%$ of the K^- absorptions occur inside the nuclear radius (i.e., defined by the radius where the nucleon density is one half of the central density). The exact fraction of d-state mesonic absorption depends sensitively on the relative nuclear capture, Auger and Stark-mixing rates in the highly excited mesonic f states. The two latter rates are difficult to estimate reliably, but it is interesting to note that if either of these were increased from the values quoted above to 10^{17} sec^{-1}, the mesonic absorption would occur almost exclusively from states with $l\leq2$, i.e., less than 20% of the captures would occur in the nuclear periphery. The fraction of d-state captures required to explain the observed multinucleon absorption of $\sim17\%$ in AgBr depends upon the degree of nucleon correlations in the regions of high density, but it appears reasonable that agreement with experiment can be obtained without invoking the nucleon-clustering model in the edge of the nucleus.

The possibility that quadrupole transitions may be a mechanism whereby nuclear absorption can occur from lower angular momentum states has also been considered. For example, when a K^- meson is in a state of large n and small l (e.g., $n\sim60$, $l\sim4$), transitions involving higher l-pole radiation might favorably compete with dipole transitions and nuclear capture. Since for these cases, $\mathbf{k}\cdot\mathbf{r}\sim1$, one might expect that the replacement of $e^{i\mathbf{k}\cdot\mathbf{r}}$ by unity in the electric-dipole approximation would not suffice. However, a calculation of the electric-quadrupole rates and of Stark-quadrupole-mixing rates shows that they are still small ($\sim4\%$) in comparison with the respective dipole rates.

ACKNOWLEDGMENTS

We gratefully acknowledge stimulating discussions with Professor W. D. Compton, Professor D. G. Ravenhall, Professor F. C. Brown, Professor J. H. Cahn, Dr. J. W. Wilkins and Dr. A. Burgess.

APPENDIX I: ELECTRON EMISSION FROM MESONIC AND HYPERONIC ATOMS

In addition to determining the electronic emission spectrum from K^--meson absorptions, a similar study of π^- absorptions was also made. By use of the short-prong method of analysis, an examination of the $2036\pi^-$ stars showed that 1181 occurred in the heavy nuclei (AgBr) and 855 were absorptions on CNO. In the heavy-nucleus events, 477 electrons of kinetic energy $\gtrsim20$ keV were observed, yielding an electron emission frequency of 0.40. (If a star yielded two electrons, both were counted.) Similarly, in the light nuclei, 30 electrons

[30] B. D. Jones, B. Sanjeevaiah, J. Zakrzewski, P. G. Bizzeti, J. P. Lagnaux, M. René, M. J. Beniston, S. A. Brown, E. H. S. Burhop, D. H. Davis, D. Ferreira, E. Frota-Pessoa, W. B. Lasich, N. N. Raina, M. C. Amerighi, A. Bonetti, M. DiCorato, C. C. Dilworth, C. A. Fedrighini, E. Quercigh, A. E. Sichirollo, and G. Vegni, Nuovo Cimento **19**, 1077 (1961); D. Evans, B. D. Jones B. Sanjeevaiah, J. Zakzrewski, M. J. Beniston, V. A. Bull, and D. H. Davis, Proc. Roy. Soc. (London) **A262**, 73 (1961); Y. Eisenberg, M. Friedmann, G. Alexander, and D. Kessler, Nuovo Cimento **22**, 1 (1961); G. T. Condo and R. D. Hill, Phys. Rev. **129**, 388 (1963).

[31] D. H. Wilkinson, in *Proceedings of the Rutherford Jubilee International Conference, Manchester, 1961* (Academic Press Inc., New York, 1961), p. 339. G. N. Fowler and A. D. Crossland, Nucl. Phys. **42**, 229 (1963).

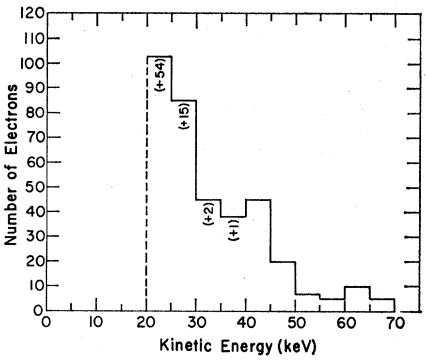

FIG. 11. Observed electron-energy spectrum (20–70 keV) for π^- mesonic atoms. An experimental cutoff was used below 20 keV. Numbers in parenthesis are to be added as corrections to the numbers already in the assigned energy bins; they represent losses attributable to the geometrical factor described in footnote (g) of Table I.

were observed for an Auger yield of ~0.04. Application of the geometrical correction, previously discussed (Sec. II), raises the heavy-nucleus electron yield to 0.47. The resulting spectrum is exhibited in Figs. 11 and 12.

A comparison of this result with the recently published data of Cuevas and Barkow[32] is difficult because of the different standards adopted by the two groups. However, the spectra displayed by the two groups are very similar in character.

Although the mesonic Auger effect for μ^- or Σ^- atoms was not investigated in the present work, we summarize briefly the work in this area. In the μ^- case, Fry,[33] in a sample of 582 μ^- captures by AgBr, found 355 associated low-energy ($\gtrsim$15 keV) electrons. Estimating the fraction of these $\gtrsim$20 keV from Fry's previous work,[34] where a spectrum was presented, we find that the μ^- electronic yield in AgBr is $\simeq$0.44 electrons per capture. However, Pevsner *et al.*,[13] in their work dealing primarily with the μ^- capture by the light elements (C, N, O) state that, in the heavy-emulsion nuclei, only $\simeq$4% of the μ^- captures are expected to yield an electron of energy between 30 and 200 keV. Thus, there appear to exist rather diverse experimental values for the electronic yield.

Finally, the data concerning Σ^- hyperic atoms are considered. These have been studied by Sacton *et al.*[35] in relationship to cryptofragment formation following nuclear Σ^- capture. In 156 definite Σ^- stars found in emulsion, 40 blobs or Auger electrons were detected. Estimating the fraction of these captures which occurred in AgBr to be ~60%, and making the extreme assumption that all of these blobs or electrons were of energy $\gtrsim$20 keV, we find that the electron yield from Σ^- hyperonic atoms is not more than 0.45.

[32] J. E. Cuevas and A. G. Barkow, Nuovo Cimento **26**, 855 (1962).
[33] W. F. Fry, Nuovo Cimento **10**, 490 (1953).
[34] W. F. Fry, Phys. Rev. **83**, 594 (1951).
[35] J. Sacton, M. J. Beniston, D. H. Davis, B. D. Jones. B. Sanjeevaiah, and J. Zakrzewski, Nuovo Cimento **23**, 702 (1962).

Table IV summarizes the experimental data and the theoretical predictions on all mesonic and hyperonic atoms.

TABLE IV. Summary of existing work on electron emission from other negative-particle atoms.

Negative particle	Theoretically assumed population at electronic K shell	Theoretical Auger intensity in AgBr (>20 keV)	Experimental electron yield in AgBr ($\gtrsim$20 keV)
Σ^-	statistical	1.10 (Ref. 2)	$\lesssim$0.45
K^-	statistical	0.81 (Ref. 2)	~0.45
π^-	statistical	0.58 (Ref. 36)	0.47
μ^-	statistical	0.61 (Ref. 37)	0.44

APPENDIX II. MESONIC-ATOM TRANSITION RATES

In order to effect the cascade calculation, the various radiative and Auger transition rates were required. Since the evaluation of matrix elements in the WKB approximation is a forbidding task, we have simplified the situation by assuming all rates can be calculated using screened hydrogenic wave functions for both the K^- meson and the electrons to be ejected. The method of derivation proceeds along standard lines first enunciated by Burhop,[19] Burbidge and de Borde,[19] and elaborated later on by de Borde,[19] DeMeur,[19] Martin,[2] and others.[36,37] Formulas for the radiative rate P_R and the K- and L-shell Auger rates, $P_A{}^K$ and $P_A{}^L$, have been given by those authors. For completeness, we have derived the Auger rates in the above approximation for the M, $N_{\mathrm{I,II,III}}$ and $N_{\mathrm{IV,V}}$ shells as well. The N shell has been divided into two parts because of the large difference in binding energy for electrons in these shells in Ag and Br. The formulas for the dipole rates of mesonic transitions $(n_1,l_1)\rightarrow(n_2,l_2)$ are listed below:

$$P_R=\frac{4e^2}{3\hbar^4c^3}\zeta_R(E_{n_1}-E_{n_2})^3\frac{\max(l_1,l_2)}{2l_1+1}|I|^2,$$

$$P_A{}^K=2\Omega(y,n_e),$$

$$P_A{}^L=(4+3y^2)(4+5y^2)\Omega(y,n_e),$$

$$P_A{}^M=(377y^8+3900y^6+4230y^4+16529y^2+6561)\Omega(y,n_e),$$

$$P_A{}^{N_{\mathrm{I,II,III}}}=(1/30)(y^2+16)\{3y^2(y^2+1)(y^2+4)\times(9y^2+80)(2304y^2+20480)+y^2(57y^4+608y^2+1280)^2+10(y^2+1)\times(11y^4+1920y^2+1536)^2\}\Omega(y,n_e),$$

$$P_A{}^{N_{\mathrm{IV,V}}}=(16/15)(y^2+16)y^4(y^2+1)(150{,}626y^4+195{,}736^2+5{,}432{,}616)\Omega(y,n_e),$$

[36] Y. Eisenberg and D. Kessler, Phys. Rev. **123**, 1472 (1961).
[37] Y. Eisenberg and D. Kessler, Nuovo Cimento **19**, 1195 (1961).

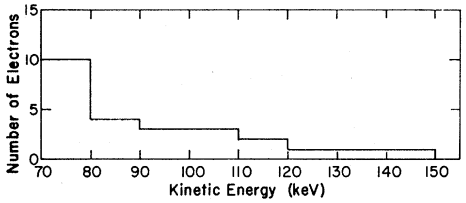

FIG. 12. Observed electron-energy spectrum (70–150 keV) for π^--mesonic atoms.

where

$$\Omega(y,n_e)=\frac{16\pi m_e e^4}{3\hbar^3}\left(\frac{Z_e}{a_0}\right)^2\zeta_A\frac{\max(l_1,l_2)}{(2l_1+1)}\frac{y^2}{(y^2+n_e^2)^{2n_e-1}}\times\frac{\exp[4y\tan^{-1}(y/n_e)-\pi y]}{\sinh\pi y}|I|^2,$$

$y=Z_e/ka_0$, Z_e is the effective nuclear charge felt by the Auger electron, and k is the momentum of the ejected electron. The integer n_e is the principal quantum number of the shell from which the electron is ejected. I is the mesonic radial dipole matrix element. ζ_R and ζ_A are enhancement factors due to the nuclear motion about the center of mass of the mesonic atom[38]; since $\zeta_R\simeq\zeta_A$, this enhancement has a negligible effect in the cascade calculation; for $n_1<16$ we find $\zeta\sim1.5$. The momentum of the ejected electron is dependent upon the electronic binding energy which was determined using Slater's screening constants.[39] It should be remarked that the approximation used to obtain the above Auger rates for mesonic transitions of energies close to the ionization limits may be oversimplified. The assumption of screened hydrogenic wave functions for such low energy electrons should be examined further.[40] However, the rates that have been determined in the calculation are for Auger electrons of sufficient energies to avoid this difficulty.

APPENDIX III: THE LEVEL SCHEME OF A K^--MESONIC SILVER ATOM

Due to the overlap of the mesonic wave function with the nucleus for low l-mesonic states and with the electronic wave functions for high n-mesonic levels, it is clear that the degeneracy of the angular momentum substates of a given level, existing for a meson in the Coulomb field of a point charge, will have been removed. Below, we investigate both these effects in turn.

A. Effects of Atomic Electron Screening

We wish to find the level scheme of highly excited mesonic states, in particular for mesonic orbits of mean radii approximately equal to that of the M-shell electrons. In this region, estimates of the K^--meson bound states based on screened hydrogenic wave functions are apt to be poor. As a better approximation, we have used Hartree-Fock electronic wave functions calculated for a free Ag^+ ion by Worsley.[21] From these wave functions the K^--meson potential energy function $V(r)$ was determined in order that the mesonic binding energies E_{nl} could be computed upon application of the WKB approximation

$$(n-l-\tfrac{1}{2})\pi\hbar=\int_{r_{\rm in}}^{r_{\rm out}}\{2m_K[-E_{nl}-V(r)]-(l+\tfrac{1}{2})^2\hbar^2/r^2\}^{1/2}dr,$$

where $r_{\rm in}$ and $r_{\rm out}$ are the classical turning points of motion. Results of these calculations are shown in Figs. 13 and 14. Table V also illustrates some of the typical results obtained from the WKB approximation; one can see, for instance, that for a binding energy of ≥1 keV, the use of screened hydrogenic wave functions for the meson would appear to be a reasonable approximation (narrow variation of n with l).

TABLE V. Values of n and l for particular K^--meson binding energies E_{nl} according to the WKB approximation for Ag^+.

E_{nl} (eV)	l	n	$r_{\rm out}$ (Å)
30	10	~141	1.0
	100	~106	0.50
350	10	~102	0.35
	50	~99	0.31
	80	~91	0.22
1000	10	~84	0.20
	30	~83	0.185
	50	~81	0.17
	70	~78	0.13

B. Effect of Finite Nuclear Size

The Coulomb potential $C_\rho(r)$ due to a Saxon-Woods shaped nucleon density distribution $\rho(r)$ was computed by numerical integration of Poisson's equation. The degeneracy of the low angular momentum mesonic substates will be removed by an energy shift due firstly to the short-range repulsive potential $C_\rho(r)\cdot Ze^2/r\equiv V_C(r)$ and secondly due to the nuclear interaction.This latter interaction may be represented by an attractive complex potential; assumed in this calculation to be $V_N(r)=U_\rho(r)$ with $U=-20$ MeV, the imaginary part of the potential was found to give only second-order changes in the energy levels and thus may be neglected in the energy-shift calculation. The exact energy levels were found

[38] Z. Fried and A. D. Martin, Nuovo Cimento **29**, 574 (1963).
[39] J. C. Slater, Phys. Rev. **36**, 57 (1930).
[40] E. H. S. Burhop, Proc. Cambridge Phil. Soc. **36**, 43 (1960), and Appendix to this paper by Professor H. S. W. Massey. Subsequent numerical calculations have been performed by W. N. Asaad and E. H. S. Burhop, Proc. Phys. Soc. (London) **71**, 369 (1958), and by W. N. Asaad, Proc. Roy. Soc. (London) **A249**, 555 (1959).

by repeated integration of the Klein-Gordon equation, matching the integrated mesonic wave function on to its appropriate analytic form for large r.[41] Typical results are given in Table VI for the $n=4$ and $n=8$

TABLE VI. Binding energies E_{nl} for K-mesonic atom, $Z=41$, $A=94$.

(i) E_{nl} (MeV) for the $n=4$ mesonic level

Potential	l: 0	1	2	3	E_{Bohr}
$V_C(r)+V_N(r)$	1.41	1.65	1.91	1.39	1.38
$V_C(r)$ alone	1.08	1.27	1.37	1.38	1.38

(ii) E_{nl} (MeV) for the $n=8$ mesonic level

Potential	l: 0	1	2	3	4	5	E_{Bohr}
$V_C(r)+V_N(r)$	0.349	0.375	0.399	0.349	0.346	0.346	0.345
$V_C(r)$ alone	0.305	0.331	0.344	0.346	0.346	0.346	0.345

levels in an $A=94$, $Z=41$ K^--mesonic atom, first for the potential $V_C(r)+V_N(r)$, and secondly for purposes of comparison just the potential $V_C(r)$ alone. It can be seen from this table, for instance, that the total energy-level shift of the $8s$-state is much less than that of the $8p$ or $8d$ due to the competing and approximately equal effects of the potentials $V_C(r)$ and $V_N(r)$ in this mesonic state. The slight difference between the $8g$, $8h$, and the Bohr level E_{Bohr} is due to the use of the Klein-Gordon equation. The general structure with respect to l shown in the table is very insensitive to the value of n, however

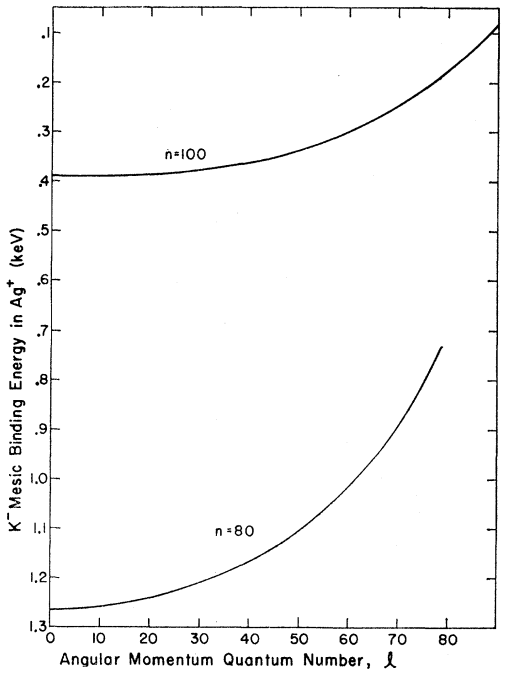

FIG. 13. Variation of binding energies of K-mesonic Ag^+ levels with angular momentum quantum number l, for a constant principal quantum number n, in the WKB approximation.

[41] A. D. Martin, Ph.D. thesis, University of London, 1962 (unpublished).

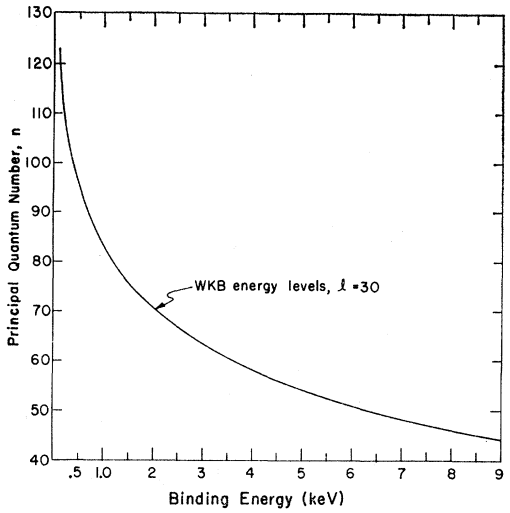

FIG. 14. Variation of binding energies of K-mesonic Ag^+ levels with principal quantum number n, for a constant angular momentum quantum number l, in the WKB approximation.

the fractional energy-level shift decreases as approximately $1/n$ as n increases.

C. Degree of Degeneracy

We are now in a position to assess the degree of degeneracy, of say, the $n=80$ mesonic level. Assuming the above nuclear potential, the increase in mesonic binding energy of the $80s$, $80p$, $80d$ substates is approximately 1, 10, 20 eV, respectively, the nuclear shifts of the $80f$ and higher angular momentum states being entirely negligible in comparison. Due to the strength of nuclear absorption, the lifetime of the K^- meson in the $80s$, $80p$, $80d$ states is less than 10^{-17} sec; thus it is seen that the corresponding broadening of these levels completely dwarfs the energy shifts and permits the Stark mixing suggested in Sec. IV B. The energy shifts arising from the screening of the nuclear charge by the atomic electrons can be seen from Fig. 13; for instance we find $\delta E_{80l}/\delta l=-1$, -2, -7, -11 eV for $l\sim 10$, 20, 40, 60, respectively.

APPENDIX IV: K^-–MESON CAPTURE REACTIONS IN Ag AND Br LEADING TO $\Sigma^\pm+\pi^\mp$+STAR CHARACTERISTICS

3-prong stars

$$(29\%)K^-+Ag^{109}\rightarrow\Sigma^\pm+\pi^\mp+p+\begin{cases} Rh^{107,107m}(1.1\%) \\ n+Rh^{106}\ (2.0\%) \\ 2n+Rh^{105,105m}(2.4\%) \\ 3n+Rh^{104,104m}(1.8\%) \\ 4n+Rh^{103,103m}(1.1\%) \end{cases}$$

$$(29\%)K^-+Ag^{107}\rightarrow\Sigma^\pm+\pi^\mp+p+\begin{cases} +Rh^{105,105m}(1.1\%) \\ n+Rh^{104,104m}(2.0\%) \\ 2n+Rh^{103,103m}(2.4\%) \\ 3n+Rh^{102}\ (1.8\%) \\ 4n+Rh^{101}\ (1.1\%) \end{cases}$$

$(21\%)K^-+\mathrm{Br}^{81}\rightarrow\Sigma^\pm+\pi^\mp+p+$
- $\mathrm{Se}^{79,79m}$ (1.1%)
- $n+\mathrm{Se}^{78}$ (2.0%)
- $2n+\mathrm{Se}^{77,77m}$ (2.4%)
- $3n+\mathrm{Se}^{76}$ (1.8%)
- $4n+\mathrm{Se}^{75}$ (1.1%)

$(21\%)K^-+\mathrm{Br}^{79}\rightarrow\Sigma^\pm+\pi^\mp+p+$
- $\mathrm{Se}^{77,77m}$ (1.1%)
- $n+\mathrm{Se}^{76}$ (2.0%)
- $2n+\mathrm{Se}^{75}$ (2.4%)
- $3n+\mathrm{Se}^{74}$ (1.8%)
- $4n+\mathrm{Se}^{73}$ (1.1%)

4-prong stars

$(29\%)K^-+\mathrm{Ag}^{109}\rightarrow\Sigma^\pm+\pi^\mp+2p+$
- $n+\mathrm{Ru}^{105}$ (0.3%)
- $2n+\mathrm{Ru}^{104}$ (0.6%)
- $3n+\mathrm{Ru}^{103}$ (0.9%)
- $4n+\mathrm{Ru}^{102}$ (1.1%)
- $5n+\mathrm{Ru}^{101}$ (1.0%)
- $6n+\mathrm{Ru}^{100}$ (0.7%)
- $7n+\mathrm{Ru}^{99}$ (0.4%)

$(29\%)K^-+\mathrm{Ag}^{107}\rightarrow\Sigma^\pm+\pi^\mp+2p+$
- $n+\mathrm{Ru}^{103}$ (0.3%)
- $2n+\mathrm{Ru}^{102}$ (0.6%)
- $3n+\mathrm{Ru}^{101}$ (0.9%)
- $4n+\mathrm{Ru}^{100}$ (1.1%)
- $5n+\mathrm{Ru}^{99}$ (1.0%)
- $6n+\mathrm{Ru}^{98}$ (0.7%)
- $7n+\mathrm{Ru}^{97}$ (0.4%)

$(21\%)K^-+\mathrm{Br}^{81}\rightarrow\Sigma^\pm+\pi^\mp+2p+$
- $n+\mathrm{As}^{77}$ (0.3%)
- $2n+\mathrm{As}^{76}$ (0.6%)
- $3n+\mathrm{As}^{75}$ (0.9%)
- $4n+\mathrm{As}^{74}$ (1.1%)
- $5n+\mathrm{As}^{73}$ (1.0%)
- $6n+\mathrm{As}^{72}$ (0.7%)
- $7n+\mathrm{As}^{71}$ (0.4%)

$(21\%)K^-+\mathrm{Br}^{79}\rightarrow\Sigma^\pm+\pi^\mp+2p+$
- $n+\mathrm{As}^{75}$ (0.3%)
- $2n+\mathrm{As}^{74}$ (0.6%)
- $3n+\mathrm{As}^{73}$ (0.9%)
- $4n+\mathrm{As}^{72}$ (1.1%)
- $5n+\mathrm{As}^{71}$ (1.0%)
- $6n+\mathrm{As}^{70}$ (0.7%)
- $7n+\mathrm{As}^{69}$ (0.4%)

5-prong stars

$(29\%)K^-+\mathrm{Ag}^{109}\rightarrow\Sigma^\pm+\pi^\mp+3p+$
- $3n+\mathrm{Tc}^{102}$ (0.2%)
- $4n+\mathrm{Tc}^{101}$ (0.5%)
- $5n+\mathrm{Tc}^{100}$ (0.7%)
- $6n+\mathrm{Tc}^{99,99m}$ (0.7%)
- $7n+\mathrm{Tc}^{98}$ (0.5%)
- $8n+\mathrm{Tc}^{97,97m}$ (0.2%)

$(29\%)K^-+\mathrm{Ag}^{107}\rightarrow\Sigma^\pm+\pi^\mp+3p+$
- $3n+\mathrm{Tc}^{100}$ (0.2%)
- $4n+\mathrm{Tc}^{99,99m}$ (0.5%)
- $5n+\mathrm{Tc}^{98}$ (0.7%)
- $6n+\mathrm{Tc}^{97,97m}$ (0.7%)
- $7n+\mathrm{Tc}^{96,96m}$ (0.5%)
- $8n+\mathrm{Tc}^{95,95m}$ (0.2%)

$(21\%)\mathrm{K}^-+\mathrm{Br}^{81}\rightarrow\Sigma^\pm+\pi^\mp+3p+$
- $3n+\mathrm{Ge}^{74}$ (0.2%)
- $4n+\mathrm{Ge}^{73,73m}$ (0.5%)
- $5n+\mathrm{Ge}^{72}$ (0.7%)
- $6n+\mathrm{Ge}^{71}$ (0.7%)
- $7n+\mathrm{Ge}^{70}$ (0.5%)
- $8n+\mathrm{Ge}^{69}$ (0.2%)

$(21\%)K^-+\mathrm{Br}^{79}\rightarrow\Sigma^\pm+\pi^\mp+3p+$
- $3n+\mathrm{Ge}^{72}$ (0.2%)
- $4n+\mathrm{Ge}^{71}$ (0.5%)
- $5n+\mathrm{Ge}^{70}$ (0.7%)
- $6n+\mathrm{Ge}^{69}$ (0.7%)
- $7n+\mathrm{Ge}^{68}$ (0.5%)
- $8n+\mathrm{Ge}^{67}$ (0.2%)